Petroleum Science (2019) 16:1403–1416
https://doi.org/10.1007/s12182-019-0332-8

ORIGINAL PAPER

Effect of overburden pressure on determination of reservoir rock types using RQI/FZI, FZI* and Winland methods in carbonate rocks

Aboozar Soleymanzadeh[1] · Saeed Parvin[1] · Shahin Kord[1]

Received: 3 November 2018 / Published online: 5 June 2019

Abstract
Rock typing is an important tool in evaluation and performance prediction of reservoirs. Different techniques such as flow zone indicator (FZI), FZI* and Winland methods are used to categorize reservoir rocks into distinct rock types. Generally, these methods are applied to petrophysical data that are measured at a pressure other than reservoir pressure. Since the pressure changes the pore structure of rock, the effect of overburden pressure on rock typing should be considered. In this study, porosity and permeability of 113 core samples were measured at five different pressures. To investigate the effect of pressure on determination of rock types, FZI, FZI* and Winland methods were applied. Results indicated that although most of the samples remain in the same rock type when pressure changes, some of them show different trends. These are related to the mineralogy and changes in pore system of the samples due to pressure change. Additionally, the number of rock types increases with increasing pressure. Furthermore, the effect of overburden pressure on determination of rock types is more clearly observed in the Winland and FZI* methods. Also, results revealed that a more precise reservoir dynamic simulation can be obtained by considering the reservoir rock typing process at reservoir conditions.

Keywords Overburden pressure · Carbonate rocks · Rock type · Reservoir quality index · Flow zone indicator · Winland method

1 Introduction

Classification of reservoir rocks into different rock types, called reservoir rock typing, is an essential tool in drilling, production and especially reservoir studies. A petrophysical rock type is presented as a group of rock samples that have similar petrophysical and geological properties that influence fluid flow (Stolz and Graves 2003). Generally, petrophysical rock typing is categorized into two separate classes which are petrophysical static rock typing (PSRT) and petrophysical dynamic rock typing (PDRT). PSRT is defined as a group of rocks with a similar capillary pressure curve in the drainage process, whereas PDRT is described as a set of rocks that shows similar fluid flow behavior (Mirzaei-Paiaman et al. 2018). Proper application of rock typing provides more real dynamic reservoir behavior in simulation models (Attar et al. 2015; Saboorian-Jooybari et al. 2015, 2016). Several techniques have been reported in the literature to determine reservoir rock types. These techniques can be classified into two general groups: the theoretical and the empirical methods. The theoretical methods (such as rock quality index (RQI)/flow zone indicator (FZI) (Amaefule and Altunbay 1993), shale zone indicator (SZI) (Jongkittinarukorn and Tiab 1997; Nooruddin and Hossain 2011), modified FZI (Nooruddin and Hossain 2011), FZI* (FZI-star) (Mirzaei-Paiaman et al. 2015) and FZI** (FZI-double star) (Mirzaei-Paiaman and Saboorian-Jooybari 2016) and PSRTI (Mirzaei-Paiaman et al. 2018)) are basically derived from the well-known Kozeny–Carman equation. Empirical methods, such as Winland (Kolodzie Jr 1980; Pittman 1992; Aguilera 2002), generate relationships between porosity, permeability and a specific size of pore throat which is taken from mercury injection capillary pressure tests.

Edited by Yan-Hua Sun

✉ Shahin Kord
sh.kord@put.ac.ir

Aboozar Soleymanzadeh
a.soleymanzadeh@put.ac.ir

Saeed Parvin
saeed.parvin.20@gmail.com

[1] Ahwaz Faculty of Petroleum, Petroleum University of Technology (PUT), Ahwaz, Iran

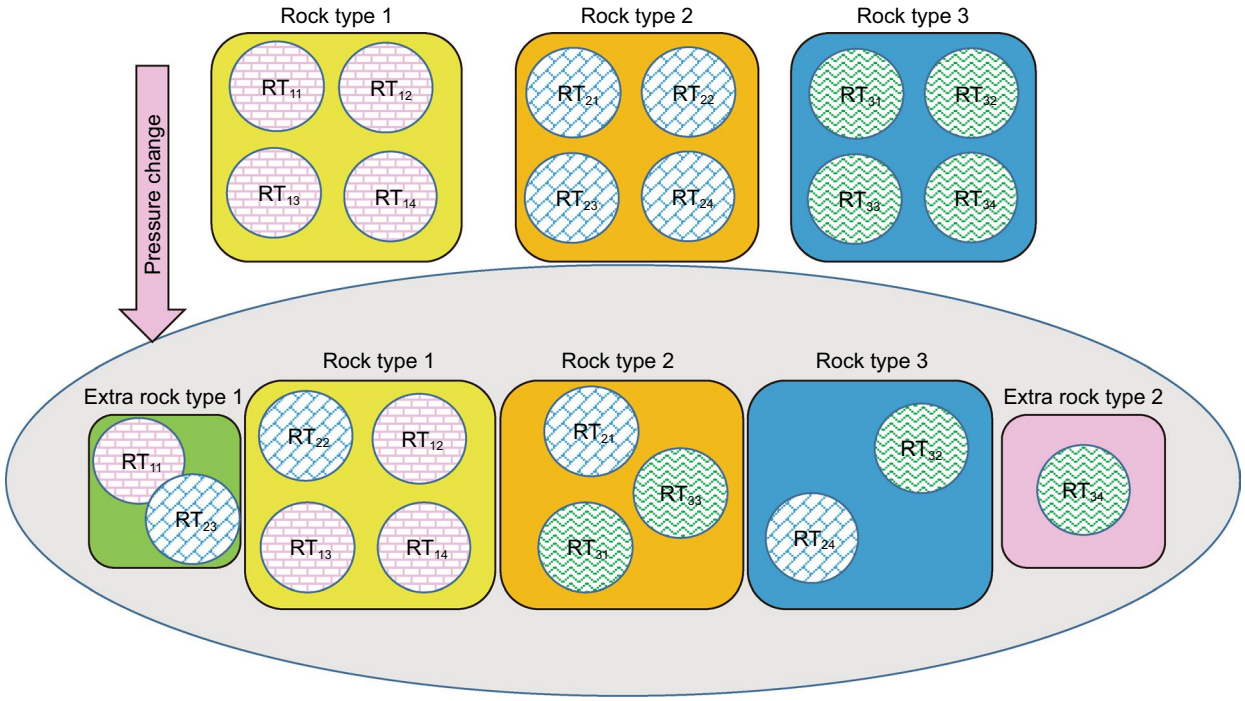

Fig. 1 Schematic of effect of pressure on rock typing process (RT1: Rock type 1, RT2: rock type 2 and RT3: rock type 3). Each circle represents a rock sample

Generally, rock typing approaches are performed at a pressure other than reservoir pressure, especially at atmospheric pressure. However, changes in pressure can alter the pore structure of the rock. When pressure is applied to different rocks, they respond differently, consequently a rock sample in a rock type that was determined at the atmospheric pressure may shift to another rock type when pressure changes (see Fig. 1). It should be noted that the effect of overburden pressure on rock is considered in commercial simulators by the rock compressibility (C_r) parameter. This parameter describes the change of porosity with pressure. However, the effect of pressure on permeability is not given as input data into the simulator. In other words, the effect of pressure on the pore structure of rock is considered by using C_r, whereas permeability and porosity change in different ways. Therefore, the effects of pressure on the process of rock type determination must be taken into consideration.

In this work, 113 core samples from one of the carbonate oil reservoirs in the Middle East have been categorized into different rock types using RQI/FZI, Winland and FZI* methods at five different pressures to investigate the effects of pressure on the process of rock type determination. It is worth mentioning that the effect of pressure in the rock typing process has not yet been investigated. In other words, most of the research examines rock type determination at a specific pressure.

In this study, first reservoir rock typing is defined. Then, three selected methods of rock typing are applied to classify studied rock samples at different overburden pressures, and finally, the results of the three methods are discussed thoroughly.

2 Reservoir rock typing

Various techniques have been suggested for classification of reservoir rocks into rock types such as the J-function method, RQI/FZI technique, capillary pressure approach and the Winland method (Soleymanzadeh et al. 2018). Among these methods, RQI/FZI and Winland approaches are the most widely used techniques of rock typing (Winland 1972; Abbaszadeh et al. 1996; Svirsky et al. 2004; Biniwale 2005; Obeida et al. 2007; Shenawi et al. 2007; Chekani and Kharrat 2009; Ye et al. 2011; Riazi 2018). However, as it is concluded from Mirzaei-Paiaman et al. (2018), the RQI/FZI method completely fails in complicated cases such as heterogeneous rocks. Therefore, they suggested that using FZI* gives more reliable results. These methods are described here briefly, and pressure effects on these techniques of rock typing are examined in following sections.

2.1 RQI/FZI approach

RQI/FZI has been derived from Kozeny–Carman equation which is based on assuming a porous medium as a bundle of capillary tubes. It is obtained by combining Poiseuille's equation and Darcy's law (Zhao et al. 2016; Chen and Yao 2017). The generalized form of the Kozeny–Carman relationship is given by the following equation:

$$k = \frac{\phi^3}{(1-\phi)^2}\left[\frac{1}{F_s \tau^2 S_{gv}^2}\right] \tag{1}$$

where k is permeability (mD), ϕ is porosity, F_s is the shape factor, τ is tortuosity, and S_{gv} is the surface area per unit grain volume.

Rearrangement of Eq. (1) results in:

$$\sqrt{\frac{k}{\phi}} = \frac{\phi}{(1-\phi)}\left[\frac{1}{\sqrt{F_s}\tau S_{gv}}\right] \tag{2}$$

Amaefule and Altunbay (1993) presented FZI as Eq. (3):

$$\mathrm{FZI} = \frac{1}{\sqrt{F_s}\tau S_{gv}} \tag{3}$$

Also, RQI is defined as follows:

$$\mathrm{RQI} = 0.0314\sqrt{\frac{k}{\phi}} \tag{4}$$

where k is permeability in mD. Normalized porosity (ϕ_z) is calculated from Eq. (5):

$$\phi_z = \frac{\phi}{1-\phi} \tag{5}$$

Substituting Eqs. (3) to (5) into Eq. (2) gives:

$$\mathrm{RQI} = \phi_z \mathrm{FZI} \tag{6}$$

Taking logarithms of both sides of Eq. (6) leads to:

$$\log \mathrm{RQI} = \log \phi_z + \log \mathrm{FZI} \tag{7}$$

where RQI and FZI are in μm, and ϕ_z is dimensionless. Equation (7) shows that a log–log plot of RQI versus ϕ_z results in a straight line with unit slope. This means that all rock samples with similar FZI value lie on an individual straight line. Therefore, the presence of different straight lines implies different rock types. Each of this rock type is denoted by its intercept at $\phi_z = 1$.

The rock typing methods were frequently used to classify reservoir rocks at atmospheric pressure. It is obvious that values of porosity and permeability in reservoir conditions are different from their values at atmospheric pressure. Therefore, using data at atmospheric pressure may result in an incorrect rock typing process and inaccurate reservoir performance prediction. A proper solution for considering pressure effect on rock type is to perform the RQI/FZI method at reservoir pressure.

2.2 Winland method

Winland performed mercury injection experiments on a large set of sandstone and carbonate rock samples to correlate porosity, permeability and the size of the pore throats. His multiple regression analysis for various mercury saturations revealed that the best correlation coefficient (R^2) is related to 35% mercury saturation. The corresponding pore throat radius of 35% mercury saturation was denoted by $r35$. The Winland correlation is as follow:

$$\log r35 = 0.732 + 0.588\log k - 0.864\log \phi \tag{8}$$

where $r35$ is in μm, k is uncorrected air permeability in mD, ϕ is porosity in percentage.

$r35$ can be used as a basis to classify a reservoir into different rock types. All rock samples with similar $r35$ constitute a single rock type and lie on an iso-pore throat curve.

2.3 FZI* method

The base form of Kozeny–Carman equation is obtained by combining Poiseuille's equation and Darcy's law, as noted in Sect. 2.1. This form of Kozeny-Carman equation is as follows:

$$k = \phi \frac{r_{mh}^2}{F_s \tau} \tag{9}$$

where r_{mh} is the effective or mean hydraulic unit radius. Mirzaei-Paiaman et al. (2015) introduced FZI* from Eq. (9):

$$\mathrm{FZI}^* = 0.0314\sqrt{\frac{k}{\phi}} \tag{10}$$

Herein, FZI* is in μm which can be calculated for each sample from measurement of its porosity and permeability. Hence, rocks with the same FZI* lie within an individual group. The fluid flow behavior of this group is assumed to be the same. Taking logarithm from both sides of Eq. (10) leads to Eq. (11).

$$\log\left(0.0314\sqrt{k}\right) = \log\sqrt{\phi} + \log \mathrm{FZI}^* \tag{11}$$

It is inferred from Eq. (11) that in a log–log scale, the plot of $0.0314\sqrt{k}$ versus $\sqrt{\phi}$ for an individual rock type shows a straight line with the slope of unity and intercept of FZI* at the $\phi = 1$.

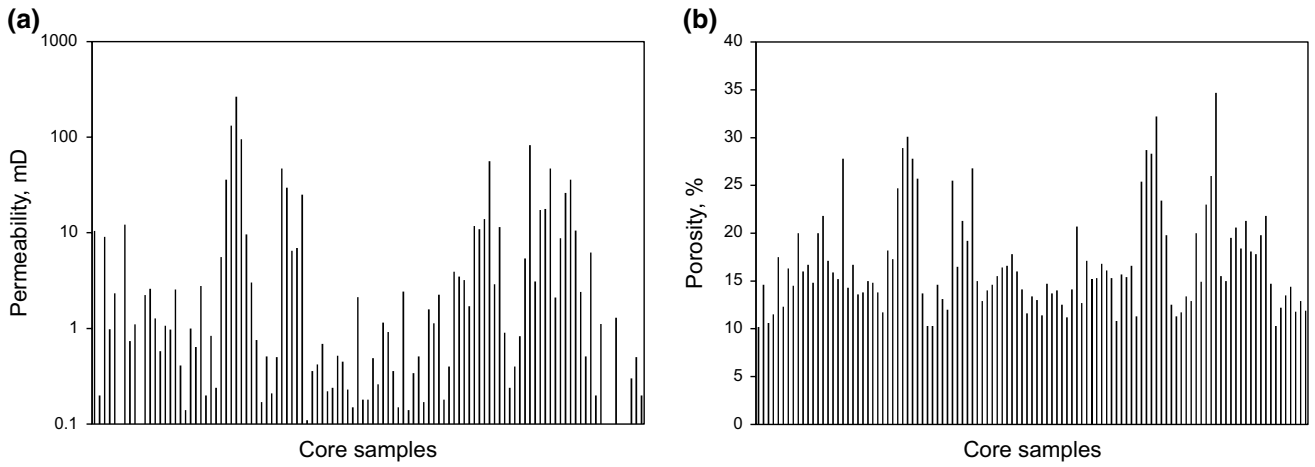

Fig. 2 Porosity and permeability of 113 core samples at atmospheric conditions

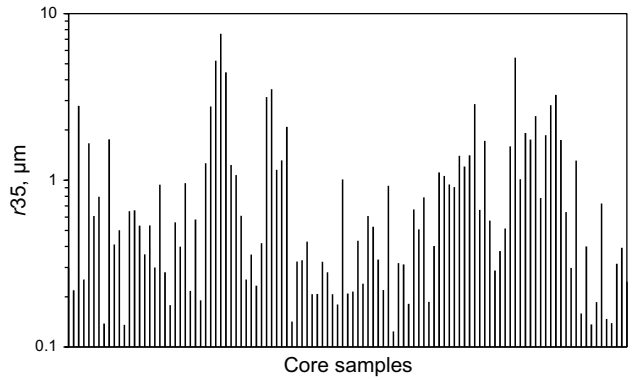

Fig. 3 *r*35 of all samples at atmospheric pressure

3 Description of rock samples

In this work, permeability–porosity data related to 113 carbonate core samples from a carbonate reservoir were used. These data have been obtained at different confining pressures (atmospheric pressure, 2000, 4000, 5000 and 6000 psia). Porosity and permeability of these rock samples at atmospheric conditions are illustrated in Fig. 2.

The value of *r*35 at atmospheric conditions is calculated for all samples from Eq. (8) (see Fig. 3).

Table 1 summarizes the average (Ave) and median (Med) of permeability, porosity and *r*35, FZI and FZI* at five different overburden pressures.

4 Results and discussion

The classical approach to reservoir rock typing, a semi-log plot of permeability versus porosity (Abbaszadeh et al. 1996), leads to undesirable results in heterogeneous reservoirs such as most carbonated reservoirs. It is noted that there is not any mathematical support for this traditional method of rock typing (Mirzaei-Paiaman et al. 2015). Fig. 4 depicts log K versus ϕ for 113 core samples at ambient pressure. This figure confirms the inappropriateness ($R^2 = 0.4882$) of the mentioned traditional technique of reservoir rock typing. Therefore, it is concluded that these data should be classified into distinct rock types.

The first step of the rock typing process is data clustering. There are different clustering techniques can be used in rock typing processes, such as discrete rock type (DRT), histogram, parabolic plots and global hydraulic element

Table 1 Average and median of porosity, permeability and *r*35 of the rock samples at different pressures

Pressure	Permeability, mD		ϕ		*r*35, µm		FZI, µm		FZI*, µm	
	Ave	Med	Ave	Med	Ave	Med	Ave	Med	Ave	Med
14.7	10.16	0.98	0.169	0.153	0.984	0.534	0.612	0.465	0.138	0.083
2000	9.54	0.7	0.153	0.139	0.947	0.538	0.626	0.460	0.131	0.080
4000	9.26	3.51	0.15	0.135	0.920	0.505	0.611	0.461	0.127	0.073
5000	9.05	0.41	0.149	0.135	0.902	0.455	0.60	0.456	0.125	0.071
6000	8.98	0.45	0.148	0.131	0.845	0.444	0.595	0.450	0.0123	0.070

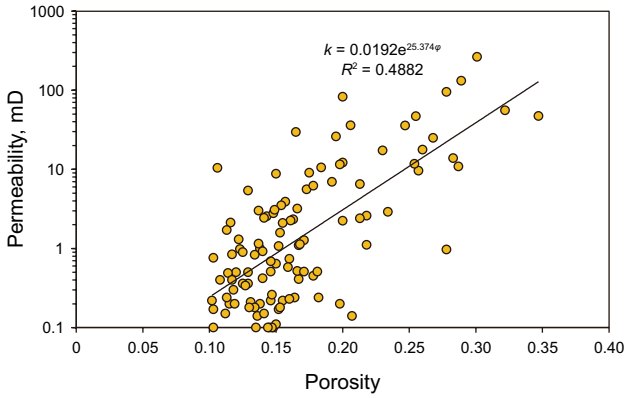

Fig. 4 Classical method of rock typing: log K versus ϕ

(Abbaszadeh et al. 1996; Corbett and Potter 2004). The DRT method was used in this work.

In order to investigate the effect of pressure on rock type determination, the RQI/FZI method was applied to determine rock types at different pressures. These rock types are illustrated in Fig. 5. Comparing rock types at different pressures reveals that the rock type of core samples changes in various ways:

a) Increasing trend (shift from lower rock type to upper one): such as core No. 51 which has been denoted by symbol▲ in Fig. 5.
b) Decreasing trend (shift from upper rock type to lower one): for example, core No. 47 which has been shown by symbol♦ in Fig. 5.
c) Fluctuating trend: such as core No. 19 which has been indicated by symbol■ in Fig. 5.
d) No change: major part of studied samples remained in the same RQI/FZI rock type.

Table 2 presents the number of samples for each mentioned trend.

In order to clarify the abovementioned trends, for each trend, some samples were selected and their FZI values were plotted versus pressure in Fig. 6. In fact, each trend in Table 2 was named according to the change in FZI value versus pressure as it is shown in Fig. 6.

Figure 7 shows the number of rock samples in each rock type. This figure reveals that the number of samples in the rock types with low values of FZI (EX1, RT7, RT8 and RT9) increased by increasing pressure. It should be emphasized that rock types EX1 and EX2 did not exist at atmospheric pressure and were added to the other rock types when pressure was increased. It means that by increasing pressure the number of rock types increases.

Since, permeability mostly depends on pore throat size rather than pore size, the authors believe that using the Winland method which contains pore throat size ($r35$) leads to a clearer description of the effect of pressure changes on the rock type determination. Whereas the RQI/FZI method is based on the Kozeny–Carman model in which the pore radius and pore throat are considered equal. In order to investigate the effect of pressure on the rock type determination by the Winland method, this method was applied to rock samples at five different pressures: 14.7, 2000, 4000, 5000 and 6000 psia (see Figs. 8, 9, 10, 11, 12).

Figures 8, 9, 10, 11 and 12 show that most of the rock samples shift to the left and downward simultaneously. In other words, this leads to change in the number of rock types and also changing a rock sample from one rock type to another one. In addition, these figures indicate that the number of data in the low k–ϕ zone (blue circle) increases with an increase in pressure.

Figure 13 depicts the number of rock samples in each of the rock types at different pressures. Three points are inferred from this figure: (1) an increase in pressure increases the number of rock types: two rock types were added to the rock types at atmospheric pressure which are indicated by EX1 and EX2 in Fig. 13. In other words, increasing pressure exacerbates the degree of heterogeneity of this dataset; (2) Increasing pressure increases the number of rock samples in the lower rock types (EX1, RT1, RT2 and RT3), and (3) for pressures greater than 4000 psia, the number of rock samples in upper rock types (RT4, RT5, RT6, EX2) remains constant.

The shift of the rock samples between different rock types (based on the Winland method) during pressure changes was examined, and results are reflected in Table 3. Indeed, Table 3 reveals that 37% of rock samples jump from one rock type to another one due to change in pressure. This means that ignoring the effect of pressure on the determination of rock types and considering k-ϕ at atmospheric pressure, make large errors in subsequent processes in a reservoir study.

Further investigations imply that 60% of rock samples which had remained in the same rock type during changes in pressure are dolomitic. This may be due to lower compressibility of dolomite rock samples with respect to limestone samples. Also, 82% of rock samples which shift from upper curves to lower curves are limestones. It should be noted that most of these samples contain vugs. It seems that the high compressibility of these vuggy limestone samples is the main reason of this trend of Table 3. A few samples (2%) jump from lower curves to upper curves which may be related to generation of fractures in the pore structure of these samples due to an increase in pressure. The fluctuating trend in Table 3 can be attributed to the generation of induced fractures and closeness of some

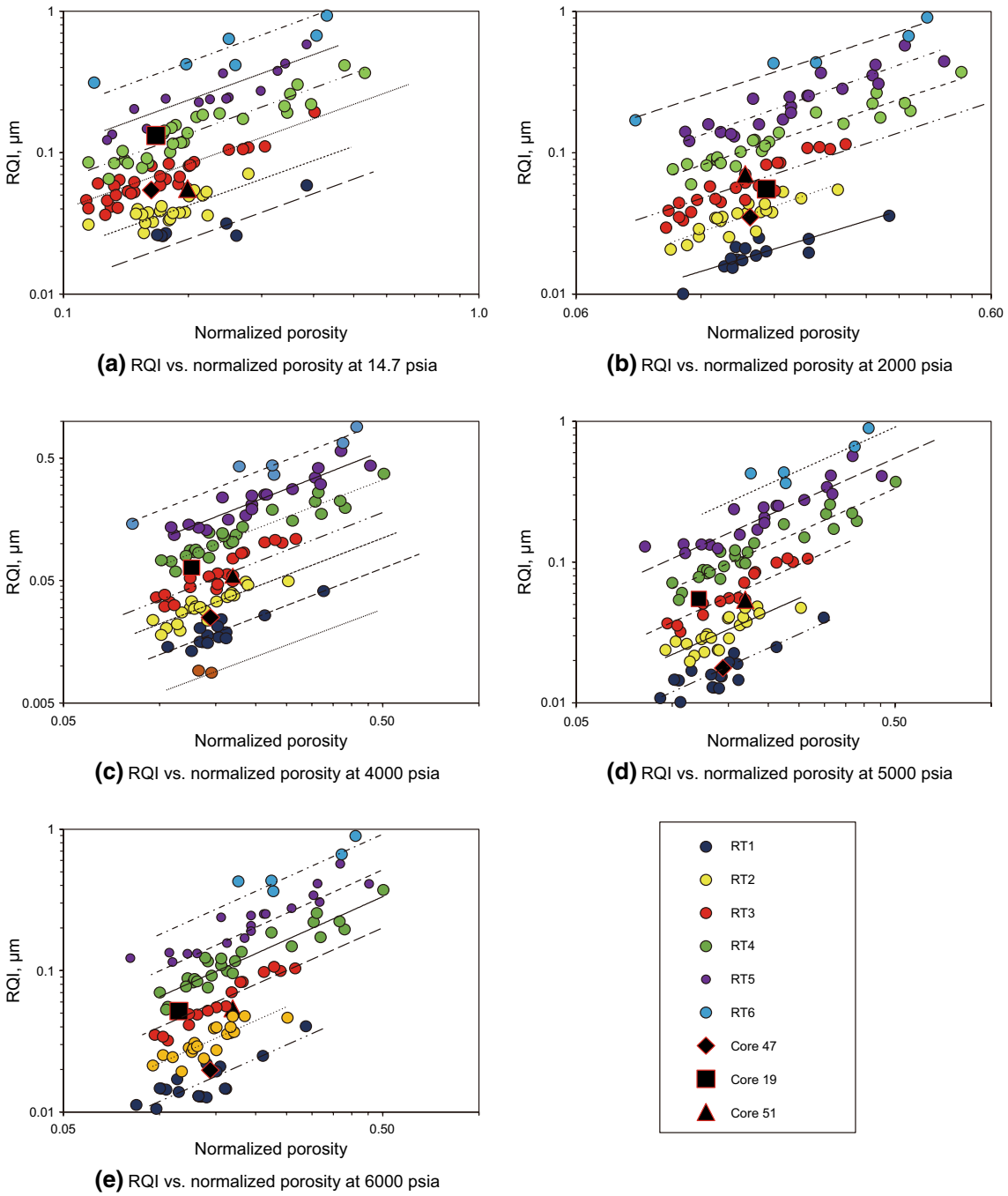

Fig. 5 RQI/FZI methods at different overburden pressures

Table 2 Four different trends due to pressure change based on the RQI/FZI method

Trend	Percentage, %	Remarks
No change	60	58% dolomite, 52% vuggy and 28% anhydrite
Increasing	10	
Decreasing	23	76% limestone, 88% vuggy
Fluctuating	7	

pores in successive steps of pressure changes. It is worth mentioning that 80% of samples with a fluctuating trend contain anhydrite. Further investigation is required to explain the effect of anhydrite content on the fluctuating trend of a rock sample. Figures 14, 15, 16 and 17 illustrate four trends of Table 3: no change, decreasing, increasing and fluctuating, respectively. In these four figures, arrow

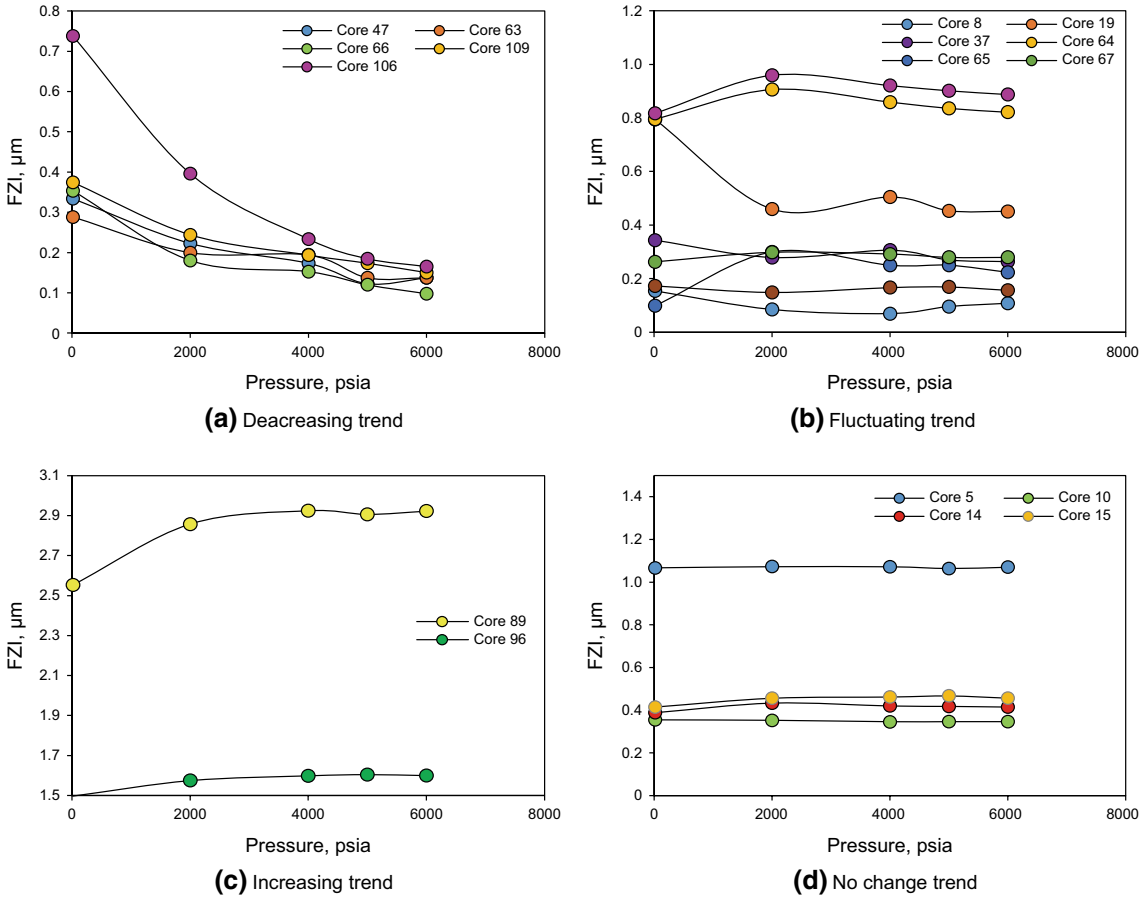

Fig. 6 Change in FZI during increasing pressure for different trends

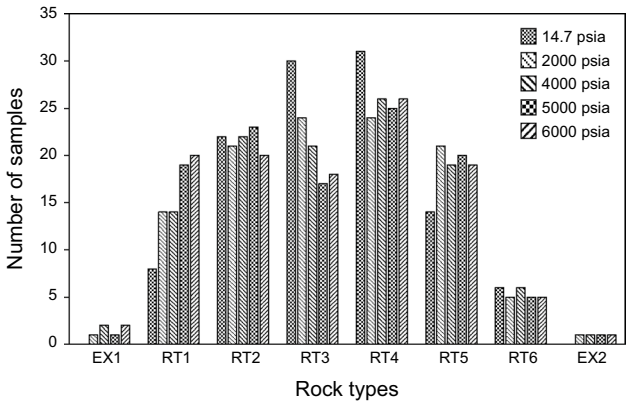

Fig. 7 Number of samples in each rock types based on the RQI/FZI method

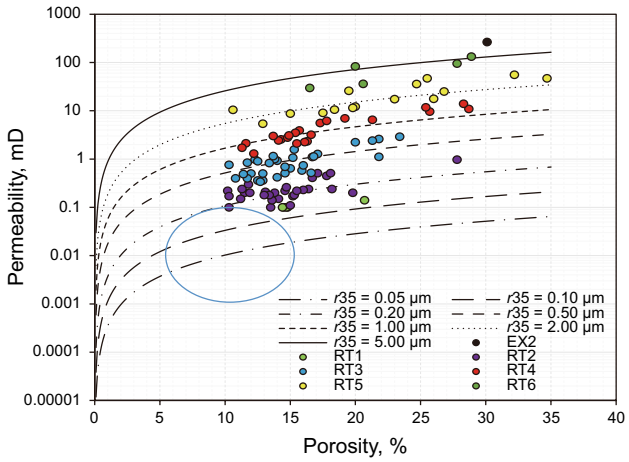

Fig. 8 Flow units based on the Winland method at 14.7 psia

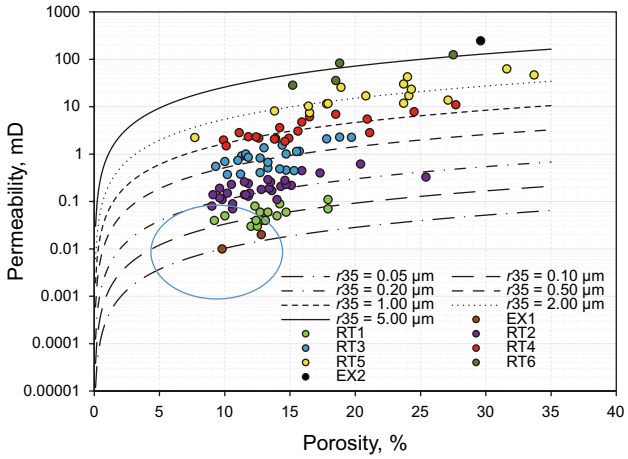

Fig. 9 Rock types based on the Winland method at 2000 psia

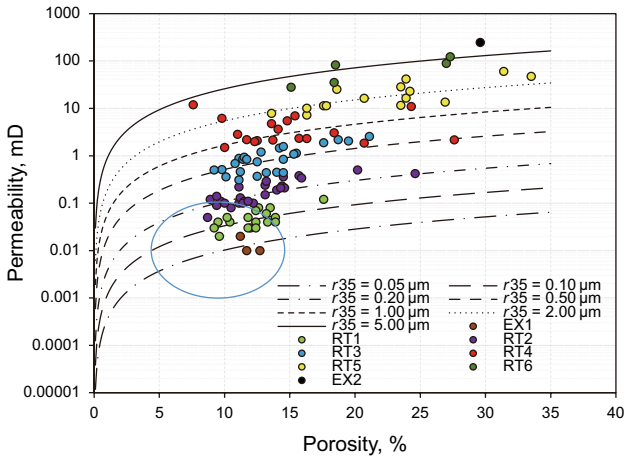

Fig. 10 Rock types based on the Winland method at 4000 psia

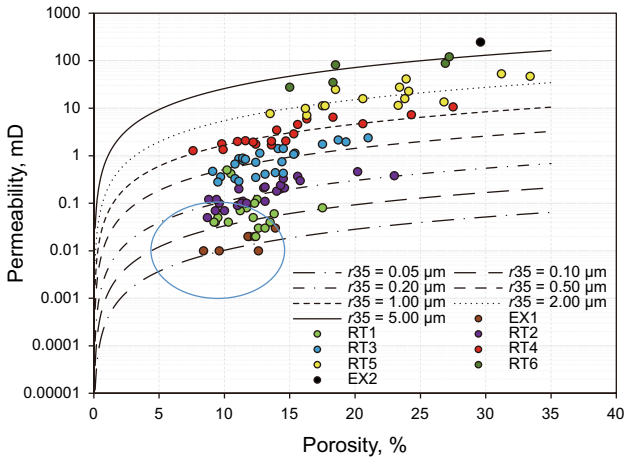

Fig. 11 Rock types based on the Winland method at 5000 psia

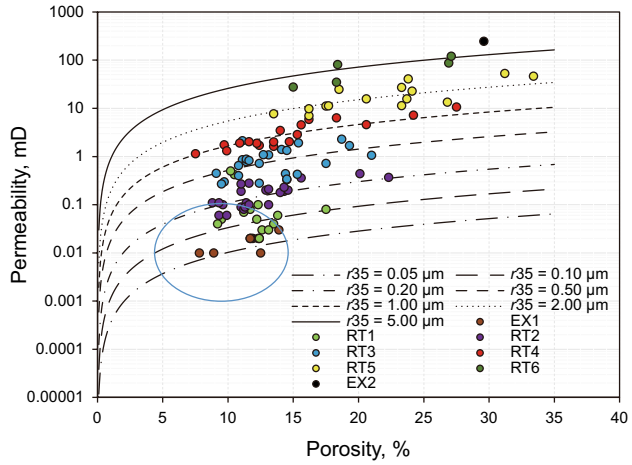

Fig. 12 Rock types based on the Winland method at 6000 psia

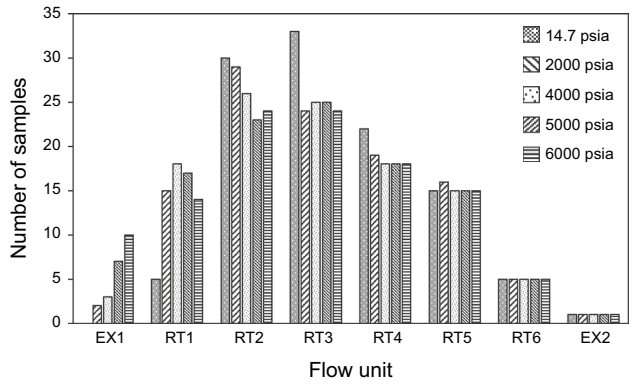

Fig. 13 Frequency of rock types based on the Winland method

Table 3 Four different trends due to pressure change based on the Winland method

Trend	Percentage, %	Remarks
No change	63	60% dolomite, 54% vuggy and 30% anhydrite
Increasing	2	
Decreasing	31	82% limestone, 81% vuggy
Fluctuating	4	80% anhydrite

direction indicates the path of change of rock types during pressure changes.

The value of *r*35 at different pressures was used to explain the observed trends in Fig. 18. This figure shows the value of *r*35 at different pressures for four different trends. (Each part of the figure is related to one trend in Table 3.) It is inferred

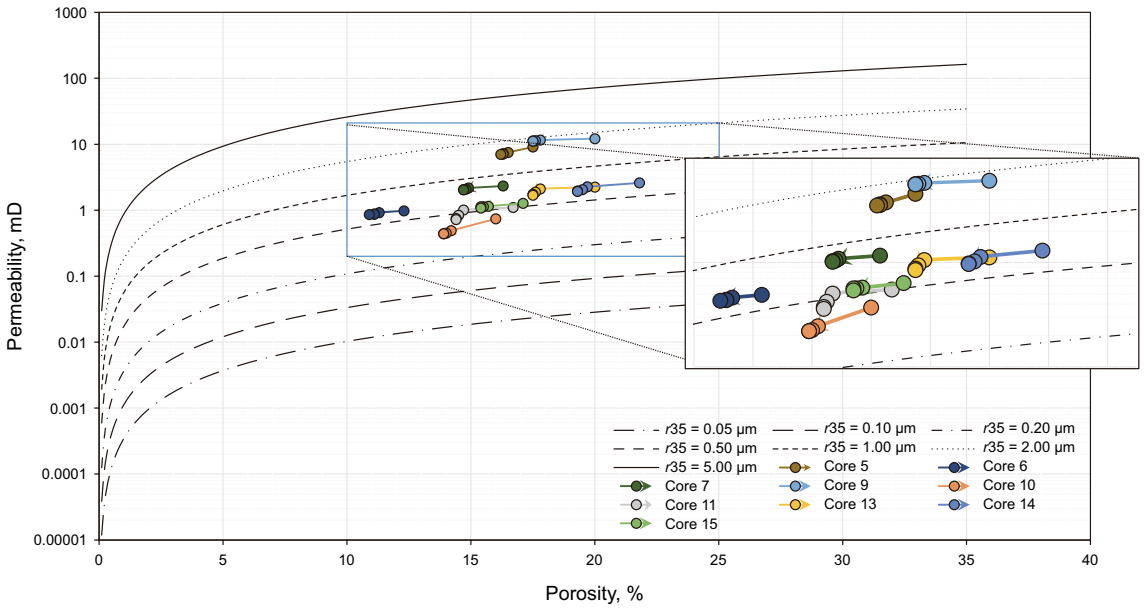

Fig. 14 Samples remain in the same rock type during pressure changes (no change trend)

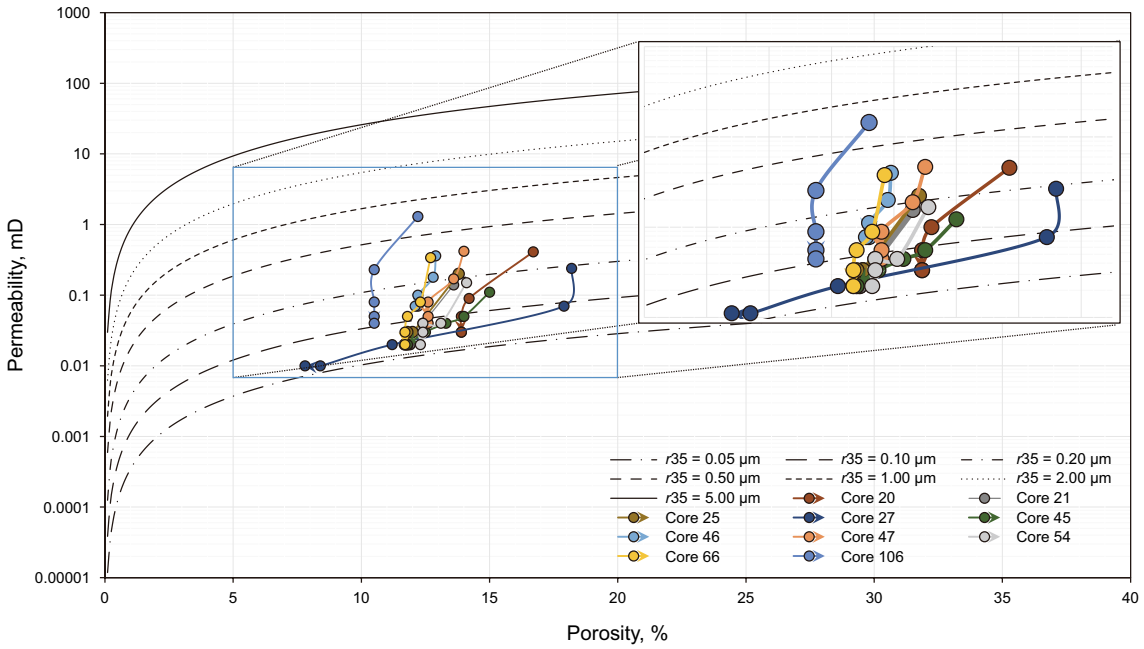

Fig. 15 Samples jump from upper curves to lower curves during pressure changes (decreasing trend)

from this figure that, all trends in Table 3 can be interpreted based on the change in *r*35 during pressure changes.

Using the FZI* method, the number of rock types increased from six to eight with an increase in overburden pressure (see Fig. 19). Rock samples move to the left and downward simultaneously, which obviously implies that the quality of the majority of the rocks reduces with an increase in pressure. Comparison of rock types at five

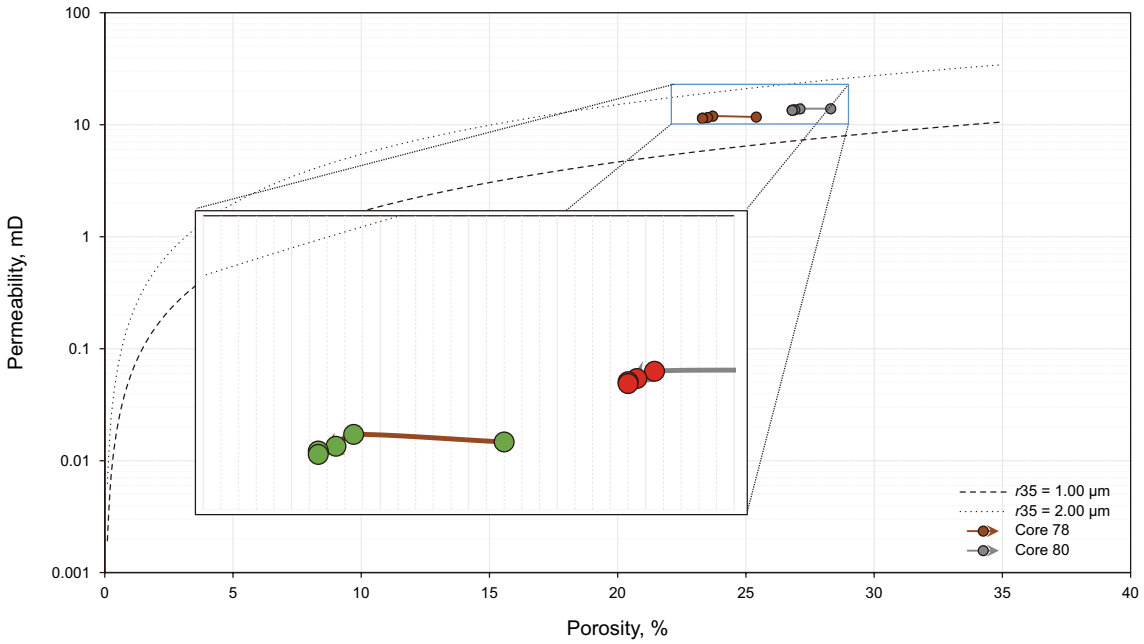

Fig. 16 Samples shift from lower curves to upper curves during pressure changes (increasing trend)

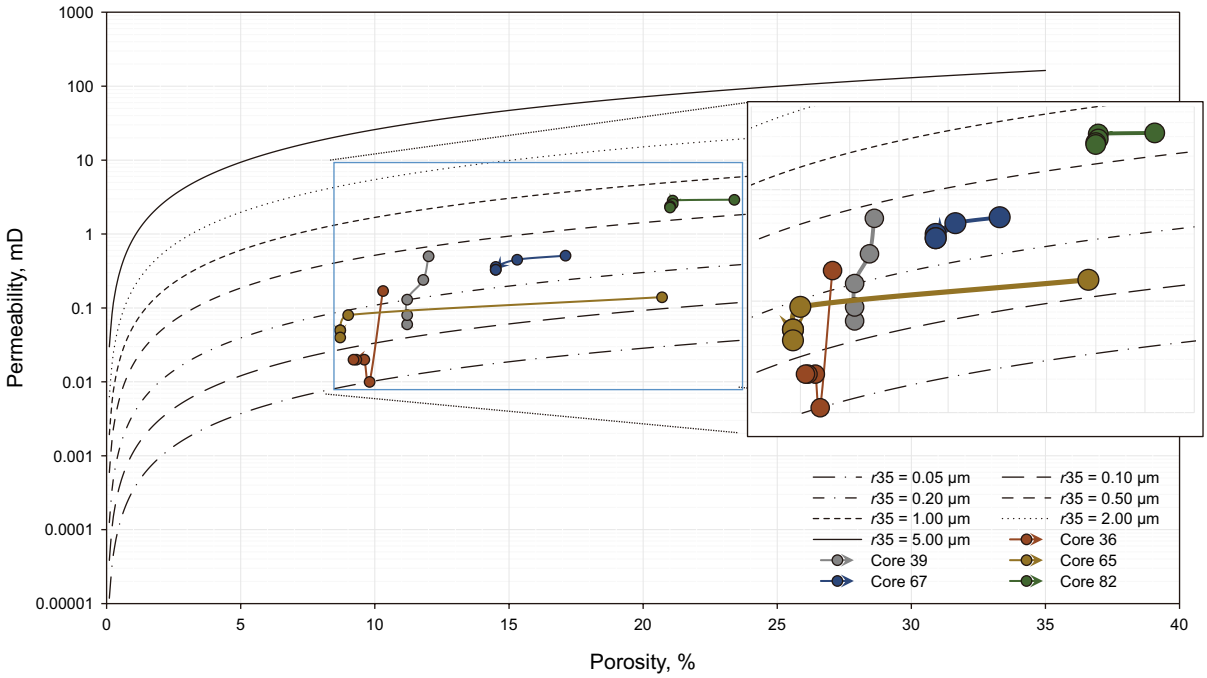

Fig. 17 Samples fluctuate between different rock types during pressure changes (fluctuating trend)

different pressures shows that rock types change in two trends: decreasing and fluctuating. Core 19 (symbol▲) and Core 65 (symbol■) represent decreasing and fluctuating trends, respectively.

The frequencies of FZI* are demonstrated in Fig. 20 which confirms the results obtained from the other two methods. Increasing pressure causes rock types EX1 and EX2 to be added to the rock types at atmospheric pressure.

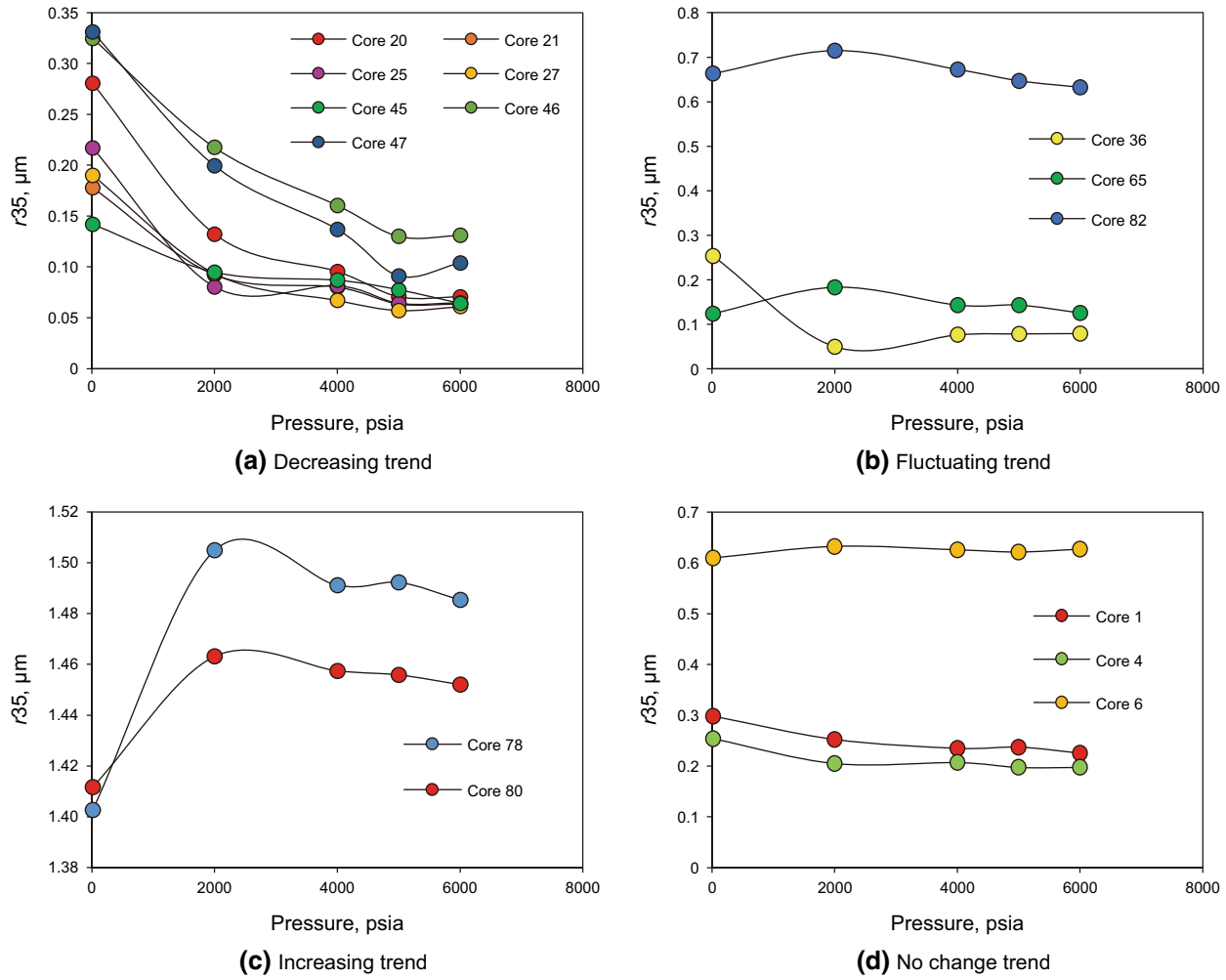

Fig. 18 r35 changes due to an increase in pressure for four different trends of Table 3

Table 4 presents the effect of pressure on the rock typing process by the FZI* method and details of observed trends due to pressure change. This table shows that, similar to RQI/FZI and Winland methods, more than 50% of studied rock samples have remained in their rock types at atmospheric pressure. Furthermore, a decreasing trend is the most common trend and vuggy limestone samples are majority of the rocks which fall within this trend, as observed in RQI/FZI and Winland methods.

Finally, it is noted that having a clearer picture of the rock pore structure, such as from micro-computed tomography (Micro-CT) scans, improves the analysis of the effect of pressure on the determination of rock types.

5 Conclusions

The following conclusions arose from this work:

(1) Studied samples were classified into different rock types using RQI/FZI, FZI* and Winland methods at five different pressures. Different behavior was observed for rock samples during changes in pressure. The majority of the samples remained in the same rock type during pressure increases. Some of the samples shifted from an upper curve to a lower curve, and a few samples change from a lower curve to an upper one. In addition, several of the rock samples showed fluctuating trends. These four different trends can be attributed to the mineralogy and change in pore structure of the studied samples.

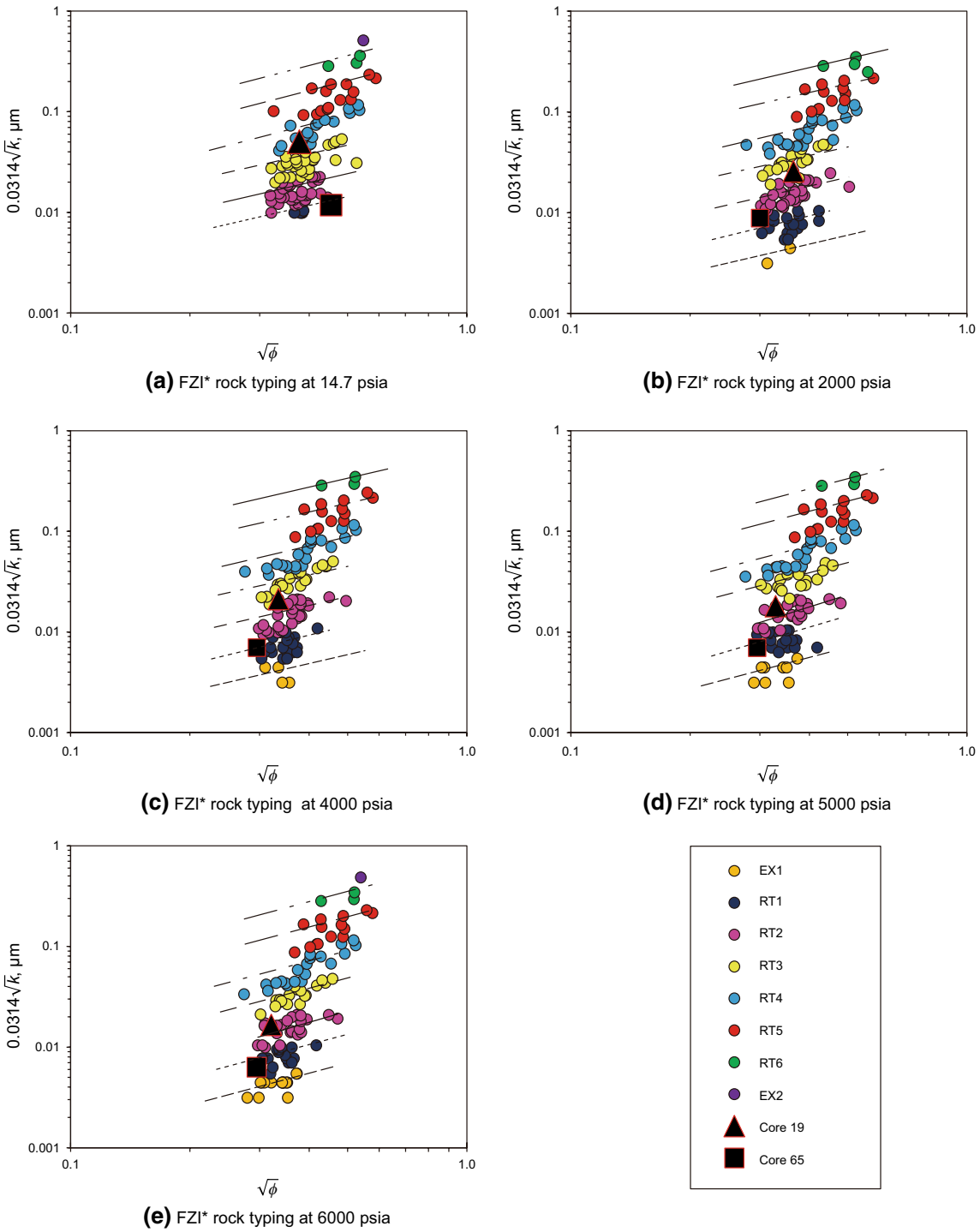

Fig. 19 Rock typing at different pressures using the FZI* method

(2) Most of the rock samples which remained in the same rock type during pressure changes are dolomitic. It seems that this is related to the lower compressibility or higher density of this type of rock. In contrary, the

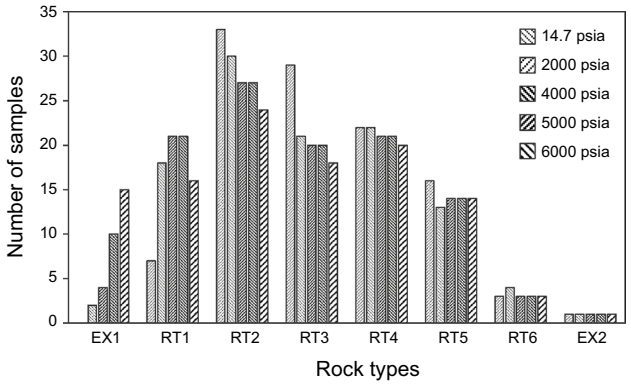

Fig. 20 Frequency of rock type based on the FZI* method

Table 4 Four different trends due to pressure change based on FZI* method

Trend	Percentage, %	Remarks
No change	55	61% dolomite, 52% vuggy and 28% anhydrite
Increasing	0	
Decreasing	42	72% limestone, 79% vuggy
Fluctuating	3	67% vuggy and 67% anhydrite

drastic changes in rock types occur in the limestone rock samples which contain vuggy porosity. The higher compressibility of these samples is the main reason of this behavior.

(3) In RQI/FZI, FZI* and Winland methods, it is observed that the number of rock types increases with an increase in pressure. Also, the number of rock samples in the lower rock types (the lower quality rock types) increases. Furthermore, generally, at pressures greater than a specific pressure (in this study, 4000 psia), the number of rock samples in the higher rock types (the higher quality rock types) remains constant.

(4) The Winland method gives a clearer picture of changing rock samples between different rock types. This is because the Winland method has been developed based on the size of pore throats ($r35$).

(5) The effect of pressure on the rock type determination implies that the process of reservoir rock typing should be performed at the reservoir conditions.

References

Abbaszadeh M, Fujii H, Fujimoto F. Permeability prediction by hydraulic flow units—theory and applications. SPE Form Eval. 1996;11(04):263–71. https://doi.org/10.2118/30158-PA.

Aguilera R. Incorporating capillary pressure, pore throat aperture radii, height above free-water table, and Winland r35 values on Pickett plots. AAPG Bull. 2002;86(4):605–24. https://doi.org/10.1306/61EEDB5C-173E-11D7-8645000102C1865D.

Amaefule JO, Altunbay M. Enhanced reservoir description using core and log data to identify hydraulic flow units and predict permeability in uncored intervals/wells. In: 68th Annual SPE conference and exhibition, 3–6 Oct Houston, Texas; 1993. https://doi.org/10.2118/26436-MS.

Attar MS, Sedaghat MH, Kord S, Mayahi H. Field development strategy through full-field reservoir simulation considering asphaltene precipitation and deposition. In: SPE reservoir characterisation and simulation conference and exhibition, 14–16 Sept, Abu Dhabi, UAE; 2015. https://doi.org/10.2118/175684-MS.

Biniwale S. An integrated method for modeling fluid saturation profiles and characterising geological environments using a modified FZI approach: Australian fields case study. In: SPE annual technical conference and exhibition, 9–12 Oct, Dallas, Texas; 2005. https://doi.org/10.2118/99285-STU.

Chekani M, Kharrat R. Reservoir rock typing in a carbonate reservoir-cooperation of core and log data: case study. In: SPE/EAGE reservoir characterization and simulation conference, 19–21 Oct, Abu Dhabi, UAE; 2009. https://doi.org/10.2118/123703-MS.

Chen X, Yao G. An improved model for permeability estimation in low permeable porous media based on fractal geometry and modified Hagen–Poiseuille flow. Fuel. 2017;210:748–57. https://doi.org/10.1016/j.fuel.2017.08.101.

Corbett P, Potter D. Petrotyping: a basemap and atlas for navigating through permeability and porosity data for reservoir comparison and permeability prediction. In: International symposium of the society of core analysts, 5–9 Oct, Abu Dhabi, UAE; 2004.

Jongkittinarukorn K, Tiab D. Identification of flow units in shaly sand reservoirs. J Pet Sci Eng. 1997;17(3–4):237–46. https://doi.org/10.1016/S0920-4105(96)00046-0.

Kolodzie Jr S. Analysis of pore throat size and use of the Waxman–Smits equation to determine OOIP in Spindle Field, CO. In: SPE annual technical conference and exhibition, 21–24 Sept, Dallas, TX; 1980. https://doi.org/10.2118/9382-MS.

Mirzaei-Paiaman A, Ostadhassan M, Rezaee R, Saboorian-Jooybari H, Chen Z. A new approach in petrophysical rock typing. J Pet Sci Eng. 2018;166:445–64. https://doi.org/10.1016/j.petrol.2018.03.075.

Mirzaei-Paiaman A, Saboorian-Jooybari H. A method based on spontaneous imbibition for characterization of pore structure: application in pre-SCAL sample selection and rock typing. J Nat Gas Sci Eng. 2016;35:814–25. https://doi.org/10.1016/j.jngse.2016.09.023.

Mirzaei-Paiaman A, Saboorian-Jooybari H, Pourafshary P. Improved method to identify hydraulic flow units for reservoir characterization. Energy Technol. 2015;3(7):726–33. https://doi.org/10.1002/ente.201500010.

Nooruddin HA, Hossain ME. Modified Kozeny–Carmen correlation for enhanced hydraulic flow unit characterization. J Pet Sci Eng. 2011;80(1):107–15. https://doi.org/10.1016/j.petrol.2011.11.003.

Obeida TA, Al-Jenaibi F, Rassas S, Serag El Din SS. Accurate calculation of hydrocarbon saturation based on log-data in complex carbonate reservoirs in the Middle-East. In: SPE/EAGE reservoir characterization and simulation conference, 28–31 Oct, Abu Dhabi, UAE; 2007. https://doi.org/10.2118/111112-MS.

Pittman ED. Relationship of porosity and permeability to various parameters derived from mercury injection-capillary pressure curves for sandstone (1). AAPG Bull. 1992;76(2):191–8.

Riazi Z. Application of integrated rock typing and flow units identification methods for an Iranian carbonate reservoir. J Pet Sci Eng. 2018;160:483–97. https://doi.org/10.1016/j.petrol.2017.10.025.

Saboorian-Jooybari H, Dejam M, Chen Z, Pourafshary P. Comprehensive evaluation of fracture parameters by dual laterolog data. J Appl Geophys. 2016;131:214–21. https://doi.org/10.1016/j.jappgeo.2016.06.005.

Saboorian-Jooybari H, Dejam M, Chen Z, Pourafshary P. Fracture identification and comprehensive evaluation of the parameters by dual laterolog data. In: SPE Middle east unconventional resources conference and exhibition, 26–28 Jan, Muscat, Oman; 2015. https://doi.org/10.2118/172947-MS.

Shenawi SH, White JP, Elrafie EA, El-Kilany KA. Permeability and water saturation distribution by lithologic facies and hydraulic units: a reservoir simulation case study. In: SPE middle east oil and gas show and conference, 11–14 March, Manama, Bahrain; 2007. https://doi.org/10.2118/105273-MS.

Soleymanzadeh A, Jamialahmadi M, Helalizadeh A, Soulgani BS. A new technique for electrical rock typing and estimation of cementation factor in carbonate rocks. J Pet Sci Eng. 2018;166:381–8. https://doi.org/10.1016/j.petrol.2018.03.045.

Stolz AK, Graves RM. Sensitivity study of flow unit definition by use of reservoir simulation. In: SPE annual technical conference and exhibition, 5–8 Oct, Denver, CO; 2003. https://doi.org/10.2118/84277-MS.

Svirsky D, Ryazanov A, Pankov M, Corbett PW, Posysoev A. Hydraulic flow units resolve reservoir description challenges in a Siberian Oil Field. In: SPE Asia Pacific conference on integrated modelling for asset management, 29–30 March, Kuala Lumpur, Malaysia; 2004. https://doi.org/10.2118/87056-MS.

Winland H. Oil accumulation in response to pore size changes, Weyburn field, Saskatchewan: Amoco Production Company Report F72-G-25, 20. p. 1972.

Ye S, Lü Z, Li R. Petrophysical and capillary pressure properties of the upper Triassic Xujiahe Formation tight gas sandstones in western Sichuan, China. Pet Sci. 2011;8(1):34–42. https://doi.org/10.1007/s12182-011-0112-6.

Zhao H, Ning Z, Zhao T, Zhang R, Wang Q. Effects of mineralogy on petrophysical properties and permeability estimation of the Upper Triassic Yanchang tight oil sandstones in Ordos Basin, Northern China. Fuel. 2016;186:328–38. https://doi.org/10.1016/j.fuel.2016.08.096.